

Impurity-Induced Electronic Nematic State and C_2 -Symmetric Nanostructures in Iron-Pnictide Superconductors

Yoshio INOUE¹, Youichi YAMAKAWA¹, and Hiroshi KONTANI¹

¹ *Department of Physics, Nagoya University and JST, TRIP, Furo-cho, Nagoya 464-8602, Japan.*
(Dated: March 12, 2021)

We propose that impurity-induced electronic nematic state is realized above the orthorhombic structure transition temperature T_S in iron-pnictide superconductors. In the presence of strong orbital fluctuations near T_S , it is theoretically revealed that a single impurity induces local orbital order with C_2 -symmetry, consistently with recent STM/STS measurements. Each impurity-induced C_2 -symmetric nanostructure aligns along a -axis by applying tiny uniaxial pressure along b -axis. In this impurity-induced nematic phase, the resistivity shows sizable in-plane anisotropy ($\rho_b/\rho_a \sim 2$) even above T_S , actually observed in various “detwinned” samples. The present study indicates the existence of strong orbital fluctuations in iron-pnictide superconductors.

PACS numbers: 74.70.Xa, 74.20.-z, 74.20.Rp

I. INTRODUCTION

Since the discovery of iron-pnictide superconductors,¹, a lot of effort has been devoted to understand the overall phase diagram, including the superconducting (SC) state in the tetragonal (T) phase and non-SC orthorhombic (O) phase. In $\text{Ba}(\text{Fe},\text{Co})_2\text{As}_2$, the O structure transition at T_S is second-order², and very large softening of shear modulus C_S suggests the existence of strong ferro-quadrupole $\phi_S \propto \hat{x}^2 - \hat{y}^2$ fluctuations above T_S ³⁻⁶. In many compounds, the superconducting (SC) transition temperature T_c takes the highest value near the endpoint of the O phase, suggesting a close relation between the superconductivity and the orbital instability. The weak ferro-quadrupole order in the O phase induces the spin-density-wave with $\mathbf{Q} = (\pi, 0)$ ⁵.

As for the SC mechanism, spin fluctuation mediated sign-reversing s -wave state (s_{\pm} -wave state) had been proposed from the early stage, noticing on the Coulomb interaction and intra-orbital nesting between hole- and electron-pockets⁷⁻⁹. In iron-pnictides, each Fermi pockets are mainly composed of t_{2g} orbitals of Fe atoms. On the other hand, orbital fluctuation mediated s -wave state without sign reversal (s_{++} -wave state) had been investigated in Refs.¹⁰⁻¹²: Strong orbital fluctuations originate from the inter-orbital nesting between Fermi pockets in the presence of Coulomb and weak electron-phonon (e -ph) interactions. The latter scenario is supported by the robustness of the SC state against impurities in many iron-pnictides¹³⁻¹⁶, and by the orbital independent SC gap observed in Ba122 systems by laser ARPES measurement^{11,17}. Also, experimental “resonance-like” hump structure in the neutron inelastic scattering is well reproduced in terms of the s_{++} -wave SC state, rather than the s_{\pm} -wave SC state, by taking the suppression in the inelastic scattering in the SC state (dissipationless mechanism)¹⁸.

According to Ref.⁵, the structure transition originates from the ferro-charge quadrupole $\phi_S = O_{x^2-y^2} \propto n_{xz} - n_{yz}$ instability, realized by the bound state formation of two orbitons with opposite momenta. By this two-

orbiton theory, we can fit the temperature dependence of C_S in $\text{Ba}(\text{Fe}_{1-x}\text{Co}_x)_2\text{As}_2$ for $x = 0 \sim 0.16$ almost perfectly¹⁹. The spin nematic theory (or two-magnon process)^{3,20} is another candidate. However, incommensurate spin order is realized in $\text{Ba}(\text{Fe}_{1-x}\text{Co}_x)_2\text{As}_2$ for $x \geq 0.056$ ²¹, although the latter theory requires commensurate fluctuations.

Furthermore, recent discovery of “electronic nematic transition” in the T phase, free from any lattice deformation, has been attracting great attention. For example, in “detwinned” $\text{Ba}(\text{Fe}_{1-x}\text{Co}_x)_2\text{As}_2$ ^{22,23} under very small uniaxial pressure ($\sim 5\text{MPa}$), sizable in-plane anisotropy of resistivity emerges at T^* , which is about $10\text{K} \sim 100\text{K}$ higher than T_S . The nematic order is also observed in $\text{BaFe}_2(\text{As},\text{P})_2$ by the magnetic torque measurement²⁴. Now, it is demanded to find which degree of freedom, spin or orbital, is more important for the nematicity, orthorhombicity and superconductivity.

In this paper, we discuss the impurity-induced electronic nematic phase in iron-pnictides, using the mean-field approximation (MFA) in real space. When orbital fluctuations develop, we obtain various types of local orbital orders with lower symmetries (C_4 , C_{2v} , C_2 , etc.), actually reported by STM/STS autocorrelation analyses^{25,26}. The large cross section of the local order gives giant residual resistivity, far beyond the s -wave unitary scattering value; $\sim 20\mu\Omega\text{cm}/\%$. When C_2 nanostructures are aligned along a -axis, the in-plane anisotropy of resistivity reaches 40%, consistently with experiments^{22,23}. Such large anisotropy is not achieved when isotropic impurity scattering is considered^{27,28}.

In annealed $\text{Ba}(\text{Fe}_{1-x}M_x)_2\text{As}_2$ ($M=\text{Co}, \text{Ni}$), the difference $|\rho_b - \rho_a|$ is very small in the absence of M -impurities ($x = 0$)²⁹, while it increases in proportional to x for $x \leq 4\%$ ^{23,29}. In contrast, both the magnetic moment and lattice deformation monotonically decrease with x . These facts strongly support the idea of impurity-induced nanostructures.

In strongly correlated electron systems, impurity potential frequently causes drastic change in the electronic state. For example, in nearly antiferromagnetic metals,

magnetic correlation is extremely enhanced near the non-magnetic impurity site, giving rise to the local magnetic moment ($\sim 1\mu_B$) and large residual resistivity³⁰ that are indeed observed in optimally- and under-doped cuprates. In terms of weak-coupling scheme, such phenomena originate from the Friedel oscillation since the large local-density-of-states (LDOS) sites could trigger the strong fluctuations around the impurity. As for the iron-based superconductors, the system would be close to antiferro-orbital critical point. Thus, it is natural to expect the occurrence of “impurity-induced local orbital order” in iron pnictides.

II. MODEL HAMILTONIAN AND METHOD OF CALCULATION

Here, we study the single-impurity problem due to orbital-diagonal impurity potential I^{10} in a large cluster with 800 Fe sites, based on the two-dimensional ten-orbital tight-binding model for LaFeAsO in Refs.^{7,31}. We set x and y axes parallel to the nearest Fe-Fe bonds. Then, the Fermi surfaces are mainly composed of t_{2g} orbitals (xz , yz and xy), although e_g orbitals also play non-negligible roles. Here, we consider the following quadrupole-quadrupole interaction^{5,10–12}:

$$H_{\text{quad}} = -g \sum_i \left\{ \hat{O}_{xz}^i \hat{O}_{xz}^i + \hat{O}_{yz}^i \hat{O}_{yz}^i + \hat{O}_{xy}^i \hat{O}_{xy}^i \right\} \quad (1)$$

where \hat{O}_Γ^i is the quadrupole operator for channel Γ at site i introduced in Ref.⁵: $\hat{O}_\Gamma^i = \sum_{l,m,\sigma} o_\Gamma^{l,m} c_{i,l\sigma}^\dagger c_{i,m\sigma}$, where $o_\Gamma^{l,m}$ is the matrix element of the charge quadrupole operator. Note that $\hat{O}_{\mu\nu} \propto \hat{l}_\mu \hat{l}_\nu + \hat{l}_\nu \hat{l}_\mu$. The quadrupole coupling constant g in eq. (1) originates from both the e -ph interaction as well as the Coulomb interaction for the charge sector, as discussed in Refs.^{10,11}. Since we are interested in the nonmagnetic orbital order, we neglect the Coulomb interaction to simplify the calculation. Then, strong orbital fluctuations for $\Gamma = xz, yz$ channels are produced by relatively small g (~ 0.2 eV)^{10–12}. Hereafter, the unit of energy is eV.

Here, we put $T = 0.02$ and the electron filling $n = 6.0$ per Fe, which corresponds to undoped compounds like BaFe₂As₂. In the absence of impurity, the bulk antiferro-orbital order occurs for $g > g_c \equiv 0.222$. Below, we study the following mean-field equation for $g < g_c$:

$$M_{l,m}^i = \langle c_{i,l\sigma}^\dagger c_{i,m\sigma} \rangle_{I,g} - \langle c_{i,l\sigma}^\dagger c_{i,m\sigma} \rangle_{I,0} \quad (2)$$

where i is the Fe site, and l, m represent the d -orbital. $M_{l,m}^i$ is impurity-induced mean-field; $\hat{M}^i = 0$ for $I = 0$. Then, the mean-field potential due to Hartree term is

$$S_{l,m}^i = \sum_{l',m'} \Gamma_{lm,l'm'}^c M_{l',m'}^i \quad (3)$$

where $\Gamma_{lm,l'm'}^c = -2g \sum_\Gamma^{xz,yz,xy} o_\Gamma^{lm} o_\Gamma^{l'm'}$ is the bare interaction for charge sector⁵, and the mean-field Hamiltonian

is $\hat{H}_{\text{MF}} = \hat{H}_0 + \sum_i \hat{S}^i + \text{const.}$ In the MFA, we solve eqs. (2)-(3) self-consistently.

III. NUMERICAL RESULTS AND DISCUSSIONS

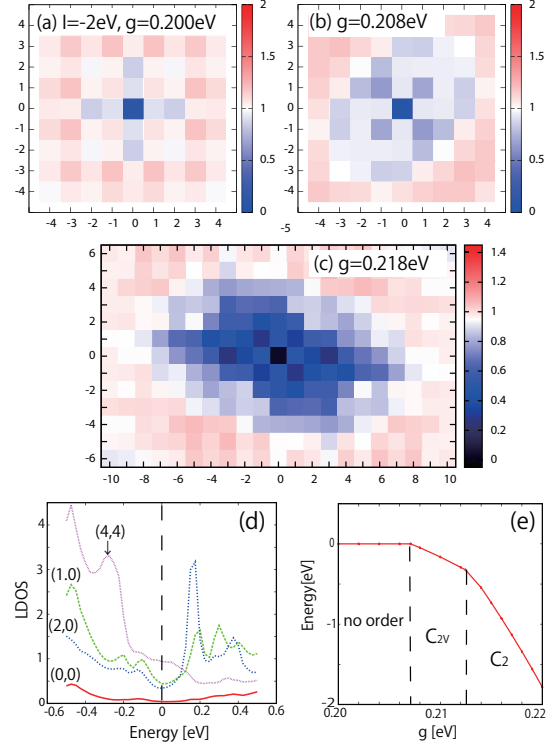


FIG. 1: (color online) Obtained LDOS at E_F for $I = -2$ and (a) $g = 0.200$: without orbital order, (b) $g = 0.208$: orbital order with diagonal C_{2v} -symmetry, and (c) $g = 0.218$: orbital order with C_2 -symmetry. (d) Energy-dependence of the LDOS for $g = 0.218$. (e) g -dependence of the free-energy.

In Figs. 1 (a)-(c), we show the obtained DOS at Fermi level (E_F) in real space, in which the center is the impurity site with $I = -2$. For $g = 0.200$ (a), the impurity-induced mean-field is absent. The small modulation of the LDOS around the impurity is caused by the Friedel oscillation. For $g > 0.207$, impurity-induced local orbital order with diagonal C_{2v} symmetry appears, as shown in (b). The suppression of the DOS is caused by the orbital order, consistently with a recent optical conductivity measurement³². With increasing g , the orbital order changes to C_2 symmetry for $g > 0.212$, shown in (c). The size of the nanostructure is $\sim 15a_{\text{Fe-Fe}}$ ($\sim 7a_{\text{Fe-Fe}}$) along x (y) axis. Such a large impurity-induced object is actually observed in Ba(Fe,Co)₂As₂ by STM/STS^{25,26}. When the impurity concentration n_{imp} is $\sim 1\%$, the obtained C_2 -order would be stabilized by the weak overlap between neighbors against thermal fluctuations omitted in the MFA. (Similar C_2 -order is also realized for $I = \infty$.) Figure 1 (d) shows the energy-dependence of LDOS for

$g = 0.218$ at $\mathbf{r} = (0,0)$ (impurity site), $(1,0)$, $(2,0)$, and $(4,4)$. Near $(0,0)$, the LDOS is modified for a wide energy range. Figure 1 (e) presents the free-energy as function of g . In the MFA, each transition at $g \approx 0.207$ and 0.212 is first-order.

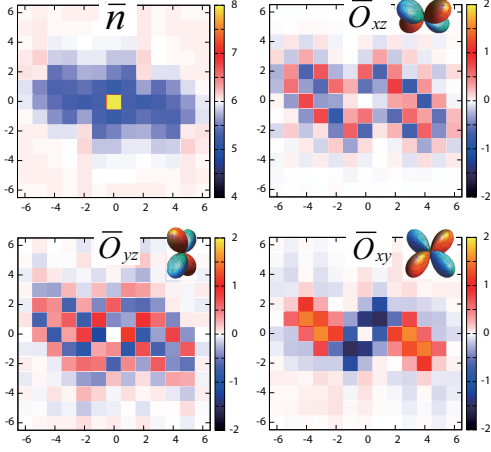


FIG. 2: (color online) Obtained electron density \bar{n}^i and quadrupole order \bar{O}_Γ^i at Fe sites for $I = -2$ and $g = 0.218$:

Since $M_{l,m}^i = M_{m,l}^i$, the present mean-field has 15 components at each site. They are represented as charge density or monopole ($l = 0$), quadrupole ($l = 2$), and hexadecapole ($l = 4$) orders. The first two orders are given as $\bar{n}^i = 2 \sum_{l,l} M_{l,l}^i$ and $\bar{O}_\Gamma^i = 2 \sum_{l,m} O_\Gamma^{l,m} M_{l,m}^i$, where $\Gamma = xz, yz, xy, z^2$, and $x^2 - y^2$. The hexadecapole order is negligibly small in the present study. Figure 2 shows the dominant four mean-fields, \bar{n}^i , \bar{O}_{xz}^i , \bar{O}_{yz}^i and \bar{O}_{xy}^i , for $g = 0.218$. We verified that the quadrupole interactions for $\Gamma = xz/yz$ channels in eq. (1) are indispensable for the C_2 -order. The obtained quadrupole order is very different from the uniform quadrupole ordered state ($\bar{O}_{x^2-y^2} \propto n_{xz} - n_{yz} = \text{const.}$) in the orthorhombic phase⁵, and therefore the impurity-induced nematic order will exist even below T_S .

The C_2 -order in Fig. 1 (c) can be aligned by the strain-induced quadrupole potential; $H' = \Delta E \sum_i \hat{O}_{x^2-y^2}^i$ and $\Delta E = \eta_S \epsilon_S \cdot \chi_{x^2-y^2}^Q(\mathbf{0}) / \chi_{x^2-y^2}^Q(\mathbf{0})$, where $\epsilon_S \propto a - b$ is the strain and η_S is the strain-quadrupole coupling. $\chi_{x^2-y^2}^Q(\mathbf{0})$ is the ferro-quadrupole susceptibility, which is strongly enhanced near T_S due to the two-orbion process as discussed in Ref.⁵. This would be the reason why the nematic ordered state is easily detwinned by small uniaxial pressure near T_S . In fact, detwinning by uniaxial pressure is possible only when the structure transition is the second-order³³.

Here, we assume $x \parallel a$ -axis and $y \parallel b$ -axis. In detwinned compounds with $a > b$, ARPES measurements indicates $\Delta E < 0$, i.e., $n_{xz} > n_{yz}$ ^{34,35}. For a single C_2 -order, we obtain the relation $F_a - F_b \approx 2.5\Delta E$, where $F_{a(b)}$ is the free-energy when the C_2 -order is along $a(b)$ -axis. Therefore, the nematic order along a -axis is realized

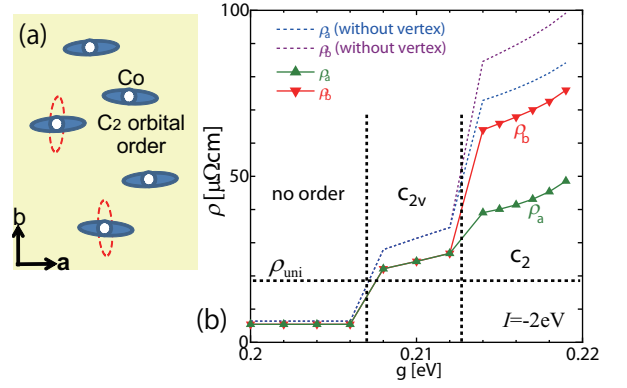


FIG. 3: (color online) (a) Alignment of the impurity-induced C_2 -orders under uniaxial pressure ($a > b$). (b) Obtained $\rho_{a(b)}$ for $n_{\text{imp}} = 1\%$ and $I = -2$: $\rho_b > \rho_a$ in the nematic phase.

by detwinning ($a > b$), schematically shown in Fig. 3 (a). Note that two kinds of C_2 -orders, the C_2 -order in Fig 1 (c) and its inversion with respect to x axis, still degenerate and coexist with equal probability.

Now, we calculate the in-plane resistivity in the nematic state shown in 3 (a). We use the T -matrix approximation, which gives the exact result when $n_{\text{imp}} \ll 1$ and localization is negligible. The T -matrix is given by solving the following equation in the orbital-diagonal basis:

$$\hat{T}_{\mathbf{r},\mathbf{r}'}(\omega) = (\hat{I} + \hat{S})_{\mathbf{r}} \delta_{\mathbf{r},\mathbf{r}'} + \sum_{\mathbf{r}''} (\hat{I} + \hat{S})_{\mathbf{r}} \hat{G}_{\mathbf{r}-\mathbf{r}''}^{(0)}(\omega) \hat{T}_{\mathbf{r}'',\mathbf{r}'}(\omega) \quad (4)$$

where $\hat{S}_{\mathbf{r}}$ is the impurity-induced mean-field potential, and $\hat{G}_{\mathbf{r}}^{(0)}(\omega)$ is the Green function without impurities. $\hat{I}_{\mathbf{r}} = I \hat{1}_{\delta_{\mathbf{r},\mathbf{0}}}$ is the impurity potential¹⁰. The T -matrix is non-local when $\hat{S}_{\mathbf{r}} \neq 0$. After the Fourier transformation, the self-energy in the T -matrix approximation is $\hat{\Sigma}(\mathbf{k},\omega) = n_{\text{imp}} \hat{T}_{\mathbf{k},\mathbf{k}}(\omega)$, and the full Green function is $\hat{G}(\mathbf{k},\omega) = (\omega + \mu - \hat{H}_{\mathbf{k}}^0 - \hat{\Sigma}(\mathbf{k},\omega))^{-1}$. Then, the in-plane conductivity is given as

$$\sigma_\nu = \frac{e^2}{\pi} \frac{1}{N} \sum_{\mathbf{k},\alpha} v_{\mathbf{k},\nu}^\alpha J_{\mathbf{k},\nu}^\alpha |G_\alpha(\mathbf{k},i\delta)|^2 \quad (5)$$

where $\nu = x$ or y , and α represents the α th band. $v_{\mathbf{k},\nu}^\alpha$ is the group velocity and $G_\alpha(\mathbf{k},\omega)$ is the full Green function in the band-diagonal basis. $J_{\mathbf{k},\nu}^\alpha$ is the total current including the vertex correction, which is given by solving the following Bethe-Salpeter equation: $J_{\mathbf{k},\nu}^\alpha = v_{\mathbf{k},\nu}^\alpha + \frac{1}{N} \sum_{\mathbf{p},\beta} I_{\mathbf{k},\mathbf{p}}^{\alpha,\beta} |G_\beta(\mathbf{p},i\delta)|^2 J_{\mathbf{p},\nu}^\beta$ where $I_{\mathbf{k},\mathbf{k}'}^{\alpha,\beta} = n_{\text{imp}} |T_{\mathbf{k},\mathbf{k}'}^{\alpha,\beta}(i\delta)|^2$ is the irreducible vertex.

The obtained results for $I = -2$ and $n_{\text{imp}} = 1\%$ are shown in Fig. 3 (b). Here, we assume the inter-layer distance is 0.6nm. Without orbital order, the resistivity is $5.5\mu\Omega\text{cm}$, which is about one-fourth of the maximum value without orbital order: $\rho_{\text{uni}} \sim 20\mu\Omega\text{cm}$ for

$I \approx +1$. When diagonal C_{2v} -order appears, the resistivity exceeds ρ_{uni} , due to large cross section of the “effective impurity radius” as recognized in Fig. 1 (b). In the nematic phase with horizontal C_2 -order, we obtain large anisotropy $\rho_b/\rho_a \sim 2$: By including the vertex correction, both ρ_a and ρ_b are suppressed and the anisotropy ρ_b/ρ_a is enlarged, since the contribution of the forward scattering is correctly subtracted. The averaged resistivity $(\rho_a + \rho_b)/2$ per 1% impurity reaches $\sim 50 \mu\Omega\text{cm}$, which is comparable to the residual resistivity by 1% Co impurities observed in La1111¹³ and Ba122²⁹.

Now, we discuss the nematic transition at T^* in real compounds. Beyond the MFA, the effective interaction \tilde{g} ($< g$) decreases with T due to the thermal fluctuation¹². Then, one possibility is that the phase transition from the diagonal C_{2v} to vertical C_2 occurs at T^* . (Then, $\tilde{g} \approx 0.212$ at T^* .) Other possibility is that C_2 order is realized even above T^* , while the necessary condition for detwinning, $\chi_{x^2-y^2}^Q(\mathbf{0}) \gg 1$, is satisfied only below T^* . In both cases, experimental results can be explained.

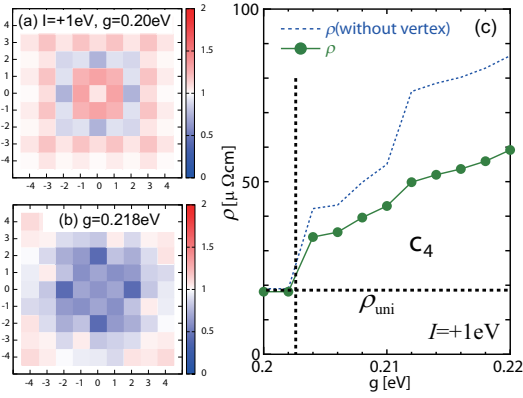


FIG. 4: (color online) Obtained LDOS at E_F in the case of $I = +1$ and (a) $g = 0.200$: without orbital order, and (b) $g = 0.218$: orbital order with C_4 symmetry. (c) Obtained resistivity for 1% impurity with $I = +1$.

We also study the impurity-induced local orbital order for $I = +1$. Figure 4 (a) shows the LDOS without orbital order: The realized Friedel oscillation pattern different from Fig. 1 (a) would induce a new type of orbital order. In fact, we obtain the orbital order with C_4 symmetry for $g > 0.203$: Figure 4 (b) shows the LDOS for $g = 0.218$. We also obtain a meta-stable solution with C_2 symmetry similar to Fig. 1 (c), whose free-energy is about 0.1 eV

higher than that for the C_4 symmetry solution. (When $I = -2$, the C_4 symmetry solution is “unstable” with positive free-energy.) Figure 4 (c) shows the resistivity $\rho = \rho_a = \rho_b$ for $I = +1$ and $n_{\text{imp}} = 1\%$: It exceeds the unitary value as soon as C_4 -order appears, and it reaches $\sim 50 \mu\Omega\text{cm}$ for $g \sim g_c$.

It is noteworthy that the obtained C_4 order looks similar to Sn-impurity-induced “ring-shape object” in LiFeAs observed by Hanaguri³⁶ very recently. The realized large reduction in the DOS would result in the suppression of the s_{++} -wave state. In fact, in BaFe_{1.89-2x}Zn_{2x}Co_{0.11}As₂, the suppression in T_c per 1% Zn-impurity is $-\Delta T_c/\% \sim 3 \text{ K}/\%$ ¹⁵: Such small suppression of T_c is consistent with the s_{++} -wave state, since $-\Delta T_c/\% \sim 20 \text{ K}/\%$ is expected in the s_{\pm} -wave state when the mass-enhancement is $m^*/m_b \sim 3$ ¹⁶.

Finally, we consider the impurities on other than Fe sites. We expect that impurity-induced nematic phase is realized in BaFe₂(As,P)₂, since P sites give finite impurity potential on the neighboring four Fe sites. In this case, we actually obtain impurity-induced order with C_2 - or C_{1h} -symmetry, consistently with experiments¹⁹. In contrast, nematic state is not realized in (K,Ba)Fe₂As₂³⁷, maybe because K sites are outside of FeAs planes.

IV. SUMMARY

In summary, we discussed impurity-induced electronic nematic state based on the orbital fluctuation theory. The obtained local orbital orders with various symmetries (C_{2v} , C_2 , and C_4) are consistent with recent STM/STS measurements. In the case of C_2 -order, the anisotropy of resistivity reaches $\rho_b/\rho_a \sim 2$, which presents a natural explanation for the nematic state in various “detwinned” iron-pnictides. Thus, characteristic features of iron pnictides, nematic and structure transitions as well as superconductivity, are well understood based on the orbital fluctuation theory.

Acknowledgments

We thank Y. Matsuda, T. Shibauchi, S. Uchida, H. Eisaki, M. Sato, M. Itoh, Y. Kobayashi, T. Hanaguri, D. Hirashima, S. Onari and T. Saito for valuable discussions. This study has been supported by Grants-in-Aid from MEXT of Japan, and by JST, TRIP.

¹ Y. Kamihara *et al.*: J. Am. Chem. Soc. **130**, 3296 (2008).

² C.R. Rotundu1 and R.J. Birgeneau, arXiv:1106.5761.

³ R.M. Fernandes, L. H. VanBebber, S. Bhattacharya, P. Chandra, V. Keppens, D. Mandrus, M.A. McGuire, B.C. Sales, A.S. Sefat, and J. Schmalian, Phys. Rev. Lett. **105**, 157003 (2010)

⁴ M. Yoshizawa, R. Kamiya, R. Onodera, Y. Nakanishi, K. Kihou, H. Eisaki, and C. H. Lee, J. Phys. Soc. Jpn. **81** (2012) 024604

⁵ H. Kontani, T. Saito, and S. Onari, Phys. Rev. B **84**, 024528 (2011): The structure transition due to two-orbital process does not require the commensurability of antiferro-

- orbitons.
- ⁶ T. Goto, R. Kurihara, K. Araki, K. Mitsumoto, M. Akatsu, Y. Nemoto, S. Tatematsu, and M. Sato, J. Phys. Soc. Jpn. **80**, 073702 (2011).
 - ⁷ K. Kuroki, S. Onari, R. Arita, H. Usui, Y. Tanaka, H. Kontani, and H. Aoki, Phys. Rev. Lett. **101**, 087004 (2008).
 - ⁸ I. I. Mazin, D. J. Singh, M. D. Johannes, and M. H. Du, Phys. Rev. Lett. **101**, 057003 (2008).
 - ⁹ P. J. Hirschfeld, M. M. Korshunov, I. I. Mazin, Rep. Prog. Phys. **74**, 124508 (2011); S. Graser, G. R. Boyd, C. Cao, H.-P. Cheng, P. J. Hirschfeld, and D. J. Scalapino, Phys. Rev. B **77**, 180514(R) (2008); A. V. Chubukov, D. V. Efremov, and I. Eremin, Phys. Rev. B **78**, 134512 (2008).
 - ¹⁰ H. Kontani and S. Onari, Phys. Rev. Lett. **104**, 157001 (2010).
 - ¹¹ T. Saito, S. Onari, and H. Kontani, Phys. Rev. B **82**, 144510 (2010).
 - ¹² S. Onari and H. Kontani, arXiv:1009.3882
 - ¹³ M. Sato, Y. Kobayashi, S. C. Lee, H. Takahashi, E. Satomi, and Y. Miura, J. Phys. Soc. Jpn. **79** (2009) 014710; S. C. Lee, E. Satomi, Y. Kobayashi, and M. Sato, J. Phys. Soc. Jpn. **79** (2010) 023702.
 - ¹⁴ Y. Nakajima, T. Taen, Y. Tsuchiya, T. Tamegai, H. Kitamura, and T. Murakami, Phys. Rev. B **82**, 220504 (2010).
 - ¹⁵ J. Li, Y. Guo, S. Zhang, S. Yu, Y. Tsujimoto, H. Kontani, K. Yamaura, and E. Takayama-Muromachi, Phys. Rev. B **84**, 020513(R) (2011).
 - ¹⁶ S. Onari and H. Kontani, Phys. Rev. Lett. **103** 177001 (2009).
 - ¹⁷ T. Shimojima, F. Sakaguchi, K. Ishizaka, Y. Ishida, T. Kiss, M. Okawa, T. Togashi, C.-T. Chen, S. Watanabe, M. Arita, K. Shimada, H. Namatame, M. Taniguchi, K. Ohgushi, S. Kasahara, T. Terashima, T. Shibauchi, Y. Matsuda, A. Chainani, and S. Shin, Science **332**, 564 (2011).
 - ¹⁸ S. Onari *et al.*, Phys. Rev. B **81**, 060504(R) (2010); S. Onari and H. Kontani, Phys. Rev. B **84**, 144518 (2011).
 - ¹⁹ H. Kontani, unpublished.
 - ²⁰ C. Fang, H. Yao, W.-F. Tsai, J. Hu, and S.A. Kivelson, Phys. Rev. B **77**, 224509 (2008).
 - ²¹ D. K. Pratt, M. G. Kim, A. Kreyssig, Y. B. Lee, G. S. Tucker, A. Thaler, W. Tian, J. L. Zarestky, S. L. Bud'ko, P. C. Canfield, B. N. Harmon, A. I. Goldman, and R. J. McQueeney, Phys. Rev. Lett. **106**, 257001 (2011)
 - ²² J.-H. Chu, J. G. Analytis, K. D. Greve, P. L. McMahon, Z. Islam, Y. Yamamoto, and I. R. Fisher, Science **329**, 824 (2010); J. J. Ying, X. F. Wang, T. Wu, Z. J. Xiang, R. H. Liu, Y. J. Yan, A. F. Wang, M. Zhang, G. J. Ye, P. Cheng, J. P. Hu, and X. H. Chen, Phys. Rev. Lett. **107**, 067001 (2011)
 - ²³ I. R. Fisher, L. Degiorgi and Z. X. Shen, Rep. Prog. Phys. **74**, 124506 (2011).
 - ²⁴ Y. Matsuda, private communication.
 - ²⁵ T.-M. Chuang, M.P. Allan, J. Lee, Y. Xie, N. Ni, S.L. Budko, G.S. Boebinger, P.C. Canfield and J.C. Davis, Science **327**, 181 (2010)
 - ²⁶ C.-L. Song, Y.-L. Wang, P. Cheng, Y.-P. Jiang, W. Li, T. Zhang, Z. Li, K. He, L. Wang, J.-F. Jia, H.-H. Hung, C. Wu, X. Ma, X. Chen, Q.-K. Xue, Science **332**, 1410 (2011).
 - ²⁷ C.-C. Chen, J. Maciejko, A. P. Sorini, B. Moritz, R. R. P. Singh, and T. P. Devereaux, Phys. Rev. B **82**, 100504(R) (2010).
 - ²⁸ R.M. Fernandes, E. Abrahams, and J. Schmalian, Phys. Rev. Lett. **107**, 217002 (2011)
 - ²⁹ M. Nakajima, T. Liang, S. Ishida, Y. Tomioka, K. Kihou, C. H. Lee, A. Iyo, H. Eisaki, T. Kakeshita, T. Ito, and S. Uchida, PNAS **108**, 12238 (2011); S. Uchida, unpublished.
 - ³⁰ H. Kontani, Rep. Prog. Phys. **71**, 026501 (2008); H. Kontani and M. Ohno, Phys. Rev. B **74**, 014406 (2006).
 - ³¹ T. Miyake, . Nakamura, R. Arita, M. Imada, J. Phys. Soc. Jpn. **79**, 044705 (2010)
 - ³² L. Stojchevska, T. Mertelj, J.-H. Chu, Ian R. Fisher, and D. Mihailovic, arXiv:1107.5934.
 - ³³ M.A. Tanatar, E.C. Blomberg, A. Kreyssig, M.G. Kim, N. Ni, A. Thaler, S.L. Budko, P.C. Canfield, A.I. Goldman, I.I. Mazin, and R. Prozorov, arXiv:1002.3801.
 - ³⁴ Q. Wang, Z. Sun, E. Rotenberg, F. Ronning, E. D. Bauer, H. Lin, R. S. Markiewicz, M. Lindroos, B. Barbiellini, A. Bansil, D. S. Dessau, arXiv:1009.0271
 - ³⁵ M. Yi, D. H. Lu, J.-H. Chu, J. G. Analytis, A. P. Sorini, A. F. Kemper, S.-K. Mo, R. G. Moore, M. Hashimoto, W. S. Lee, Z. Hussain, T. P. Devereaux, I. R. Fisher, Z.-X. Shen, PNAS **108** 6878.
 - ³⁶ T. Hanaguri, unpublished.
 - ³⁷ J. J. Ying, X. F. Wang, T. Wu, Z. J. Xiang, R. H. Liu, Y. J. Yan, A. F. Wang, M. Zhang, G. J. Ye, P. Cheng, J. P. Hu, and X. H. Chen, Phys. Rev. Lett. **107**, 067001 (2011)